Defense Threat Reduction Agency
8725 John J. Kingman Road, MS 6201
Fort Belvoir, VA 22060-6201

DTRA-TR-13-58

TECHNICAL REPORT

Processing and Dynamic Failure Characterization of Novel Impact Absorbing Transparent Interpenetrating Polymer Networks (*t*-IPN)

February 2014

HDTRA1-09-1-0023

Dr. Hareesh V. Tippur and
Dr. Maria L. Auad

Prepared by:
Auburn University
310 Samford Hall
Auburn, AL 36849

DESTRUCTION NOTICE:

Destroy this report when it is no longer needed.
Do not return to sender.

PLEASE NOTIFY THE DEFENSE THREAT REDUCTION AGENCY, ATTN: DTRIAC/ J9STT, 8725 JOHN J. KINGMAN ROAD, MS-6201, FT BELVOIR, VA 22060-6201, IF YOUR ADDRESS IS INCORRECT, IF YOU WISH THAT IT BE DELETED FROM THE DISTRIBUTION LIST, OR IF THE ADDRESSEE IS NO LONGER EMPLOYED BY YOUR ORGANIZATION.

REPORT DOCUMENTATION PAGE

Form Approved
OMB No. 0704-0188

1. REPORT DATE *(DD-MM-YYYY)*	**2. REPORT TYPE**	**3. DATES COVERED** *(From - To)*
00-02-2012	Technical	April 1, 2009 - March 31, 2013

4. TITLE AND SUBTITLE

Processing and Dynamic Failure Characterization of Novel Impact Absorbing Transparent Interpenetrating Polymer Networks (t-IPN)

5a. CONTRACT NUMBER
HDTRA1-09-1-0023

5b. GRANT NUMBER

5c. PROGRAM ELEMENT NUMBER

6. AUTHOR(S)
Dr. Hareesh V. Tippur and Maria L. Auad

5d. PROJECT NUMBER

5e. TASK NUMBER

5f. WORK UNIT NUMBER

7. PERFORMING ORGANIZATION NAME(S) AND ADDRESS(ES)
Auburn University
310 Samford Hall
Auburn, AL 36849

8. PERFORMING ORGANIZATION REPORT NUMBER

9. SPONSORING / MONITORING AGENCY NAME(S) AND ADDRESS(ES)
Defense Threat Reduction Agency
8725 John J. Kingman Road STOP 6201
Fort Belvoir, VA 22060
PM/Calvin Shipbaugh/BE-BCR

10. SPONSOR/MONITOR'S ACRONYM(S)
DTRA

11. SPONSOR/MONITOR'S REPORT NUMBER(S)
DTRA-TR-13-58

12. DISTRIBUTION / AVAILABILITY STATEMENT
Approved for public release; distribution is unlimited.

13. SUPPLEMENTARY NOTES

14. ABSTRACT

IPNs were synthesized with polyurethane (PU) and methacrylate-based polymers to create transparent materials with high toughness for potential impact loading applications. It has four parts with the fourth involving successful synthesis of IPNs based on PU and poly(methyl methacrylate) (PMMA). Other aspects included: aliphatic vs. aromatic isocyanates in the PU phase, the presence of an inhibitor in the PMMA phase (sequential vs. simultaneous reactions), curing profiles, and ratios of PU:PMMA. Samples that included an iliphatic isocyanate and a sequential polymerization demonstrated the best material properties.

IPNS with PMMA:PU ratios in the range of 90:10 to 70:30 were mechanically characterized. Dynamic fracture test and low-velocity impact test were performed. Dynamic fracture and impact responses show that an optimum PMMA:PU ratio in the IPNs produce enhanced fracture toughness (~40%) and energy impact absorption (~300%) relative to PMMA. Fractography shows phase inversion associated with improved macroscale dynamic properties.

15. SUBJECT TERMS

interpenetrating polymer networks, transparent armor, impact and fracture resistance, high strain rate behavior

16. SECURITY CLASSIFICATION OF:			**17. LIMITATION OF ABSTRACT**	**18. NUMBER OF PAGES**	**19a. NAME OF RESPONSIBLE PERSON**
a. REPORT	**b. ABSTRACT**	**c. THIS PAGE**	SAR	28	Calvin Shipbaugh
Unclassified	Unclassified	Unclassified			**19b. TELEPHONE NUMBER** *(include area code)* 703-767-3182

Standard Form 298 (Rev. 8-98)
Prescribed by ANSI Std. Z39.18

CONVERSION TABLE

Conversion Factors for U.S. Customary to metric (SI) units of measurement.

MULTIPLY →	BY →	TO GET
TO GET ←	BY ←	DIVIDE

angstrom	1.000 000 x E -10	meters (m)
atmosphere (normal)	1.013 25 x E +2	kilo pascal (kPa)
bar	1.000 000 x E +2	kilo pascal (kPa)
barn	1.000 000 x E -28	meter^2 (m^2)
British thermal unit (thermochemical)	1.054 350 x E +3	joule (J)
calorie (thermochemical)	4.184 000	joule (J)
cal (thermochemical/cm^2)	4.184 000 x E -2	mega joule/m^2 (MJ/m^2)
curie	3.700 000 x E +1	*giga bacquerel (GBq)
degree (angle)	1.745 329 x E -2	radian (rad)
degree Fahrenheit	$t_k = (t^\circ f + 459.67)/1.8$	degree kelvin (K)
electron volt	1.602 19 x E -19	joule (J)
erg	1.000 000 x E -7	joule (J)
erg/second	1.000 000 x E -7	watt (W)
foot	3.048 000 x E -1	meter (m)
foot-pound-force	1.355 818	joule (J)
gallon (U.S. liquid)	3.785 412 x E -3	meter^3 (m^3)
inch	2.540 000 x E -2	meter (m)
jerk	1.000 000 x E +9	joule (J)
joule/kilogram (J/kg) radiation dose absorbed	1.000 000	Gray (Gy)
kilotons	4.183	terajoules
kip (1000 lbf)	4.448 222 x E +3	newton (N)
kip/inch^2 (ksi)	6.894 757 x E +3	kilo pascal (kPa)
ktap	1.000 000 x E +2	newton-second/m^2 ($N-s/m^2$)
micron	1.000 000 x E -6	meter (m)
mil	2.540 000 x E -5	meter (m)
mile (international)	1.609 344 x E +3	meter (m)
ounce	2.834 952 x E -2	kilogram (kg)
pound-force (lbs avoirdupois)	4.448 222	newton (N)
pound-force inch	1.129 848 x E -1	newton-meter (N-m)
pound-force/inch	1.751 268 x E +2	newton/meter (N/m)
pound-force/foot^2	4.788 026 x E -2	kilo pascal (kPa)
pound-force/inch^2 (psi)	6.894 757	kilo pascal (kPa)
pound-mass (lbm avoirdupois)	4.535 924 x E -1	kilogram (kg)
pound-mass-foot^2 (moment of inertia)	4.214 011 x E -2	kilogram-meter^2 ($kg-m^2$)
pound-mass/foot^3	1.601 846 x E +1	kilogram-meter^3 (kg/m^3)
rad (radiation dose absorbed)	1.000 000 x E -2	**Gray (Gy)
roentgen	2.579 760 x E -4	coulomb/kilogram (C/kg)
shake	1.000 000 x E -8	second (s)
slug	1.459 390 x E +1	kilogram (kg)
torr (mm Hg, 0^0 C)	1.333 22 x E -1	kilo pascal (kPa)

*The bacquerel (Bq) is the SI unit of radioactivity; 1 Bq = 1 event/s.

**The Gray (GY) is the SI unit of absorbed radiation.

Objectives:

List the objectives of the research effort or the statement of work: This may be omitted if there has been no change. State new or revised objectives if they have changed and the reason why.

1) Develop novel *transparent* Interpenetrating Polymer Networks (*t*-IPNs),
2) Enhance *t*-IPNs with different PU network morphologies,
3) Reinforce *t*-IPNs with functionalized silica particles generated in situ,
4) Engineer interphase between the IPN phases and the filler for optimum rigidity and toughness,
5) Characterize the performance of the material under shock and impact loading conditions

Status of Effort:

A brief statement of progress towards achieving the research objectives. (Limit to 200 words).

This project began in April 2009, and since August 2009, transparent IPN (*t*-IPN) systems based on polyurethane (PU) and poly(methyl methacrylate) (PMMA) have been synthesized and characterized. The inclusion of silica particles has also been studied. More recently, the effect of altering the PU network morphology and its effects on the final IPN morphology and material properties has been investigated. High-strain rate fracture behavior of PU/PMMA t-IPNs have been carried out and compared with the corresponding quasi-static tests.

Accomplishments:

The purpose of this research is to enhance the mechanical performance of currently available materials used for transparent armor and to create a material that can compete with technology currently on the market. During the first part of this study, optically *t*-IPNs, based on PU/PMMA, were synthesized and characterized. From the results and observations made after every step during this section, it was found that interpenetrated PU/PMMA materials appeared to have promising roles both as a monolithic armor material and as a backing material in a layered architecture.

Different IPN formulations were prepared and characterized during the first part of this research. The chemicals used for PU preparation were: poly(tetramethylene ether) glycol (PTMG), 2,4-toluene diisocyanate (TDI), 1,1,1-tris(hydroxymethyl) propane (TRIOL), and dibutyltin dilaurate (DD), where this chemical was used as a catalyst. Additionally 1,6-diisocyanatohexane (DCH) was investigated for replacing TDI. The chemicals used for PMMA were: methyl methacrylate (MMA), trimethylpropane trimethacrylate (TRIM), and azobisisobutyro nitrile (AIBN). Ethyl acetate was also used as a non-polymerizable analogue to the AIBN and the DD.

IPNs Consisting of PMMA:PU

Several problems were addressed in the beginning of the research, and much time was spent on analyzing the various parameters in the systems. The first feature investigated was the effect of adjusting the PU/PMMA ratio and the changes in thermo-mechanical properties, morphology, and phase separation. The effect of different heat treatments, or the changes produced when post-curing did or did not take place, was also investigated. Despite a marginal increase in the Young's modulus (E') and thermal properties, this was not enough to compensate for the development of less transparent IPNs. Additionally, two separate isocyanates were used for the synthesis of the PU phase, TDI and DCH. After preparing several samples, it was found that a yellow color was produced from the aromatic TDI; DCH, an aliphatic isocyanate, produced clear IPNs. Another parameter that was studied was the effect of using an inhibitor in the PMMA phase, or in other words, the effect of having a sequential versus a simultaneous IPN. It was found that simultaneous IPNs exhibited extreme phase separation, not conducive to this study.

Figure 1 shows transmission electron microscopy (TEM) photos of 80:20 IPNs (PMMA:PU) with either DCH or TDI in the PU phase, as well as pure PMMA, each stained with osmium tetroxide. It was found that the PMMA phase remained transparent while the PU phase absorbed the dye. Using this information, it was possible to distinguish between the two phases under the microscope. Samples consisting of DCH generally display a homogeneous grey color, indicating that phase separation was minimal. On the other hand, samples containing TDI clearly show patches of dark grey or white, especially in Figure 1d, correlating to major phase separation within the IPN.

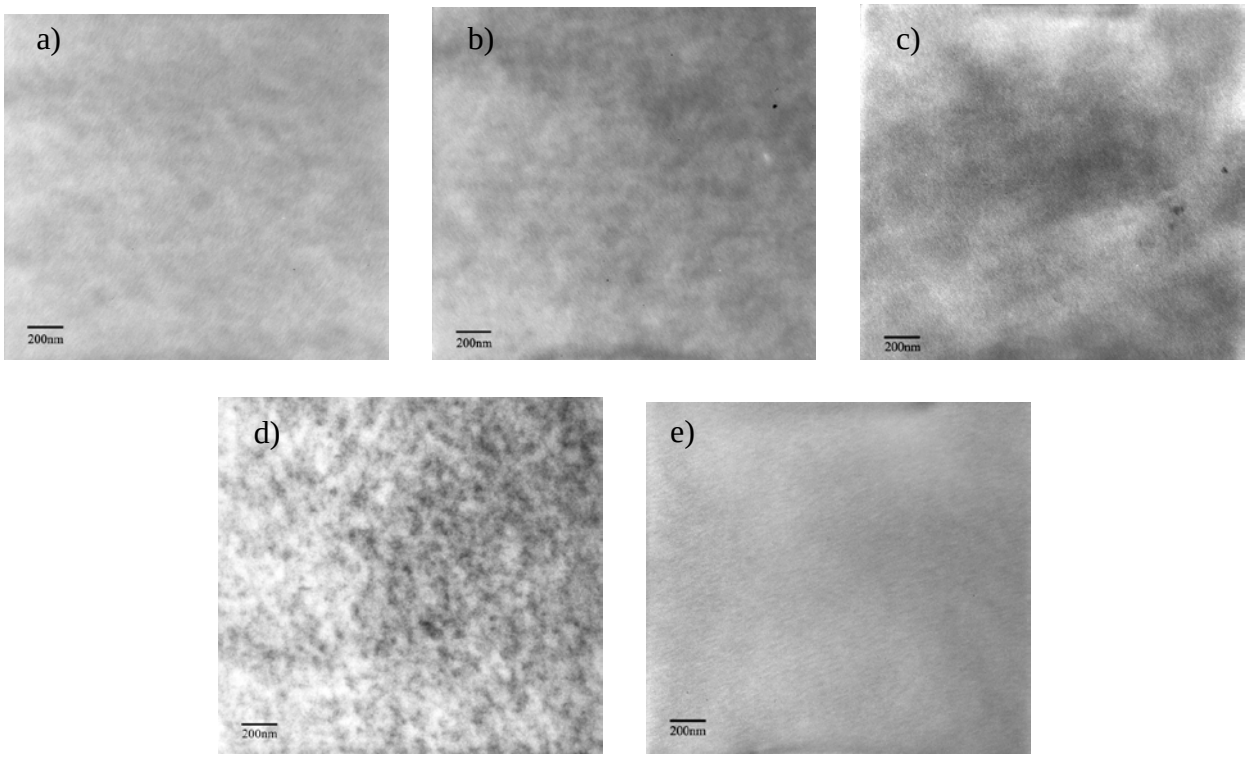

Figure 1. TEM photos of IPNs with 80wt% PMMA with a) an inhibitor and DCH, b) an inhibitor and TDI, c) no inhibitor and DCH, d) no inhibitor and TDI, and e) pure PMMA with inhibitor

Results from UV-visible spectrophotometry (UV-vis) analysis in Figure 2 show the effects of using DCH or TDI in the IPNs.

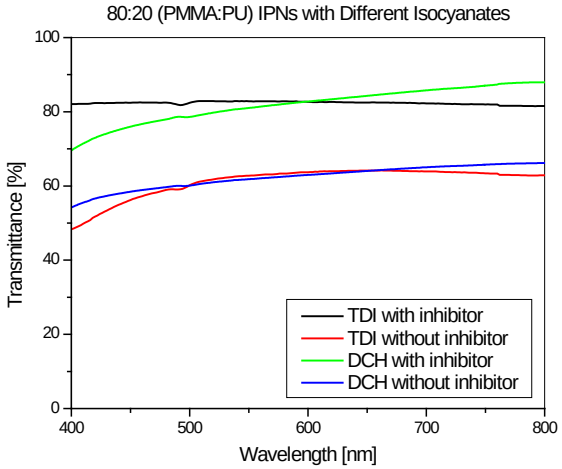

Figure 2. UV-visible results showing IPNs consisting of 80 wt% PMMA and 20 wt% PU with different isocyanates

As can be seen in the graph above, the transparency was greatly reduced when TDI was included in the PU phase. This corresponds not only to the yellow discoloration that was observed and discussed earlier, but the phase separation seen in the TEM photos also lowered the transparency of the IPNs.

Figure 3 shows SEM photos of commercial PMMA, PU synthesized with DCH, and IPNs synthesized with DCH in the PU phase that were broken under liquid nitrogen. By breaking at this temperature, it was possible to observe the morphology of the samples when failure occurred. As can be seen, samples consisting of either 80:20 or 70:30 (PMMA:PU) exhibited a higher degree of surface area, corresponding to a potentially higher degree of impact absorbance.

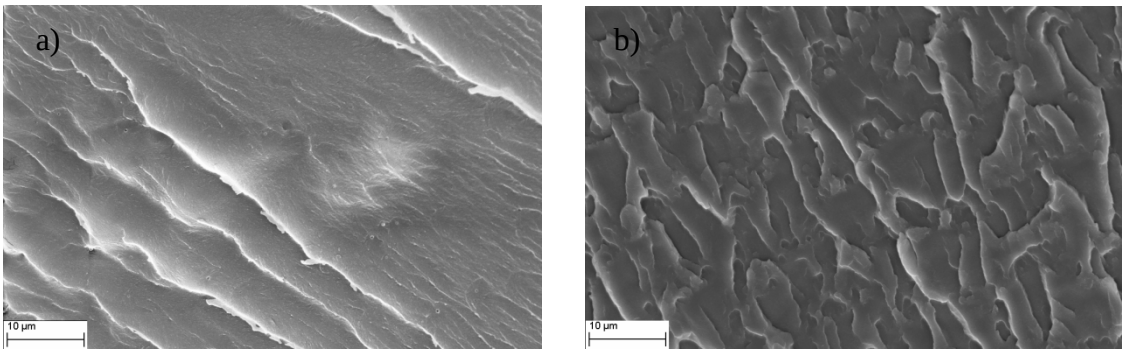

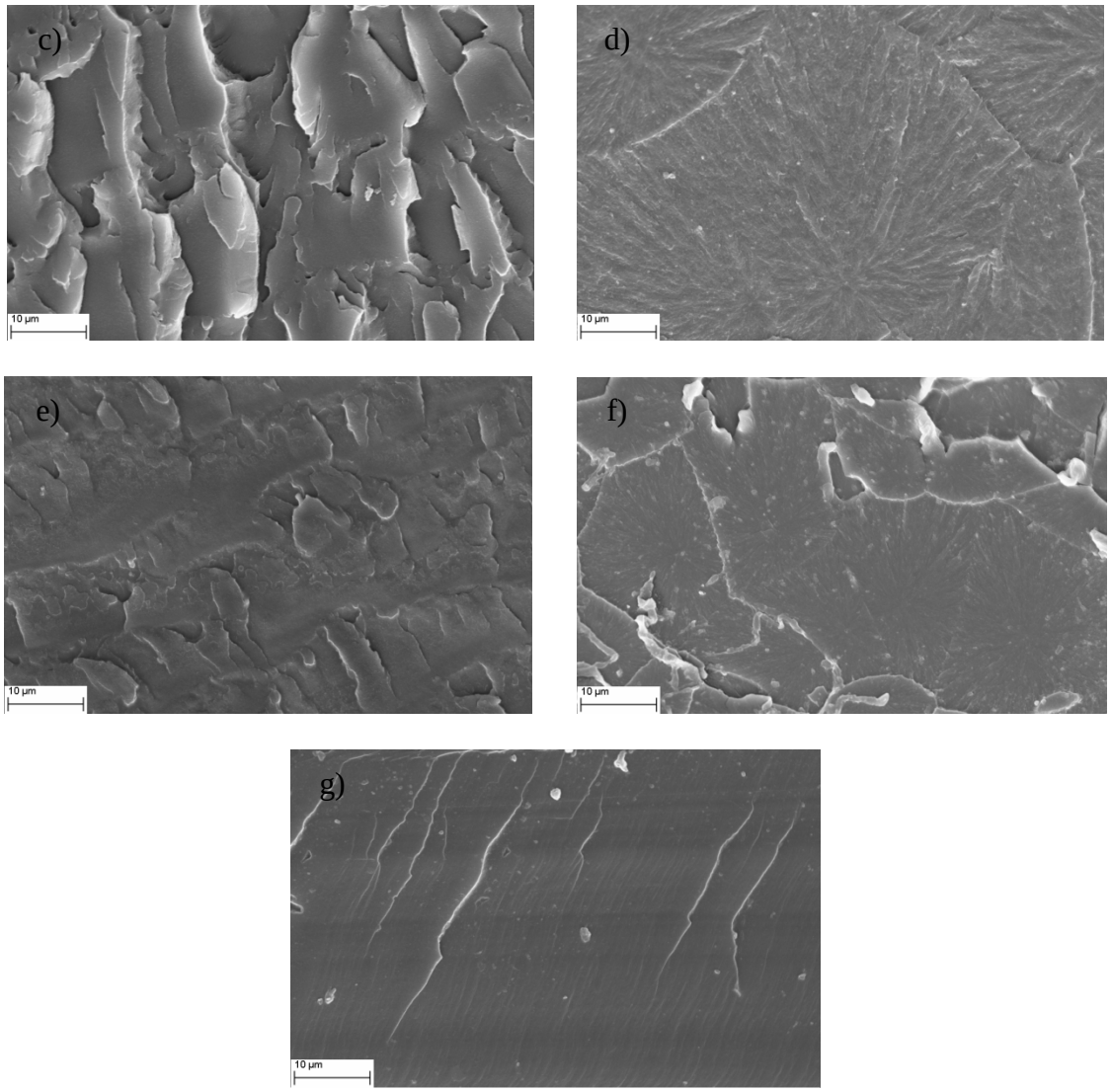

Figure 3. SEM photos of a) commercial PMMA, IPNs with an inhibitor, DCH, and b) 80 wt% PMMA c) 70 wt% PMMA d) 60 wt% PMMA e) 50 wt% PMMA, f) 40 wt% PMMA, and g) pure PU with DCH

Thermo-mechanical and fracture properties were also investigated for this research. For the thermo-mechanical tests, dynamic mechanical analysis (DMA) as used. Figures 4a and 4b show the E' and tan δ values, respectively, of IPNs with DCH, an inhibitor present in the PMMA phase, and different ratios of PMMA:PU. For E', the values decreased as more of the PU phase was included in the IPN. This was expected since adding more of the soft, rubbery phase in the IPN would make the material more ductile. On the other hand, including more of the rigid PMMA phase created stiffer samples.

The T_g, or the peak of the tan δ curves, also increased when higher amounts of PMMA were included in the IPNs. PMMA has a higher T_g than PU, so having more of this phase would shift the peak of the tan δ curve, or the T_g, to higher temperatures. All tan δ curves exhibited one peak which was indicative of the presence of minimal phase separation.

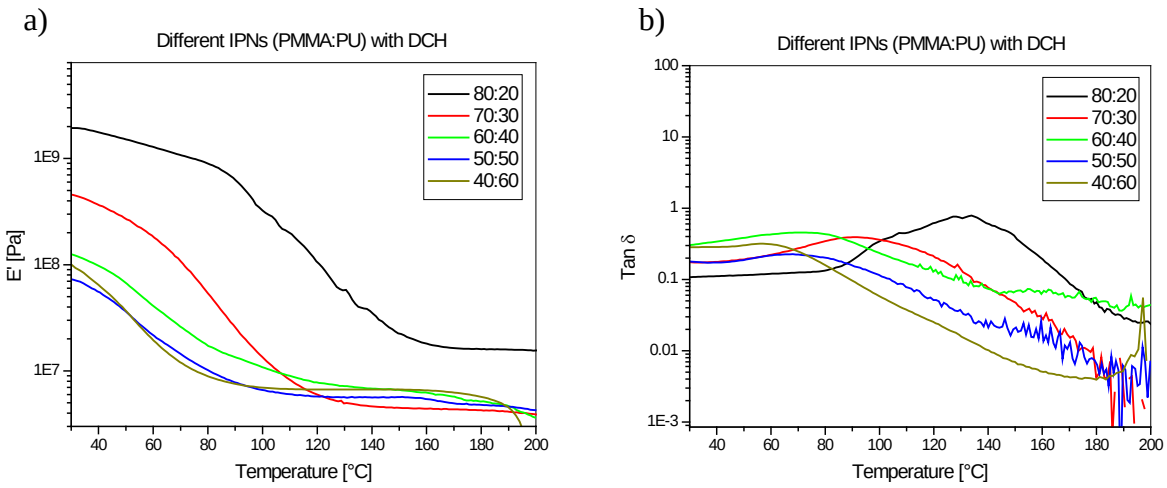

Figure 4. E' and Tg values of IPNs with DCH, an inhibitor present in the PMMA phase, and with different ratios of PMMA:PU

Mechanical Characterization

Dynamic fracture behavior of PU-PMMA IPNs has been carried out to complement the static tensile and fracture responses reported in the last report. In addition, work on impact energy absorption by IPN compositions has also been initiated and currently underway.

In the following details on these aspects are briefly described:

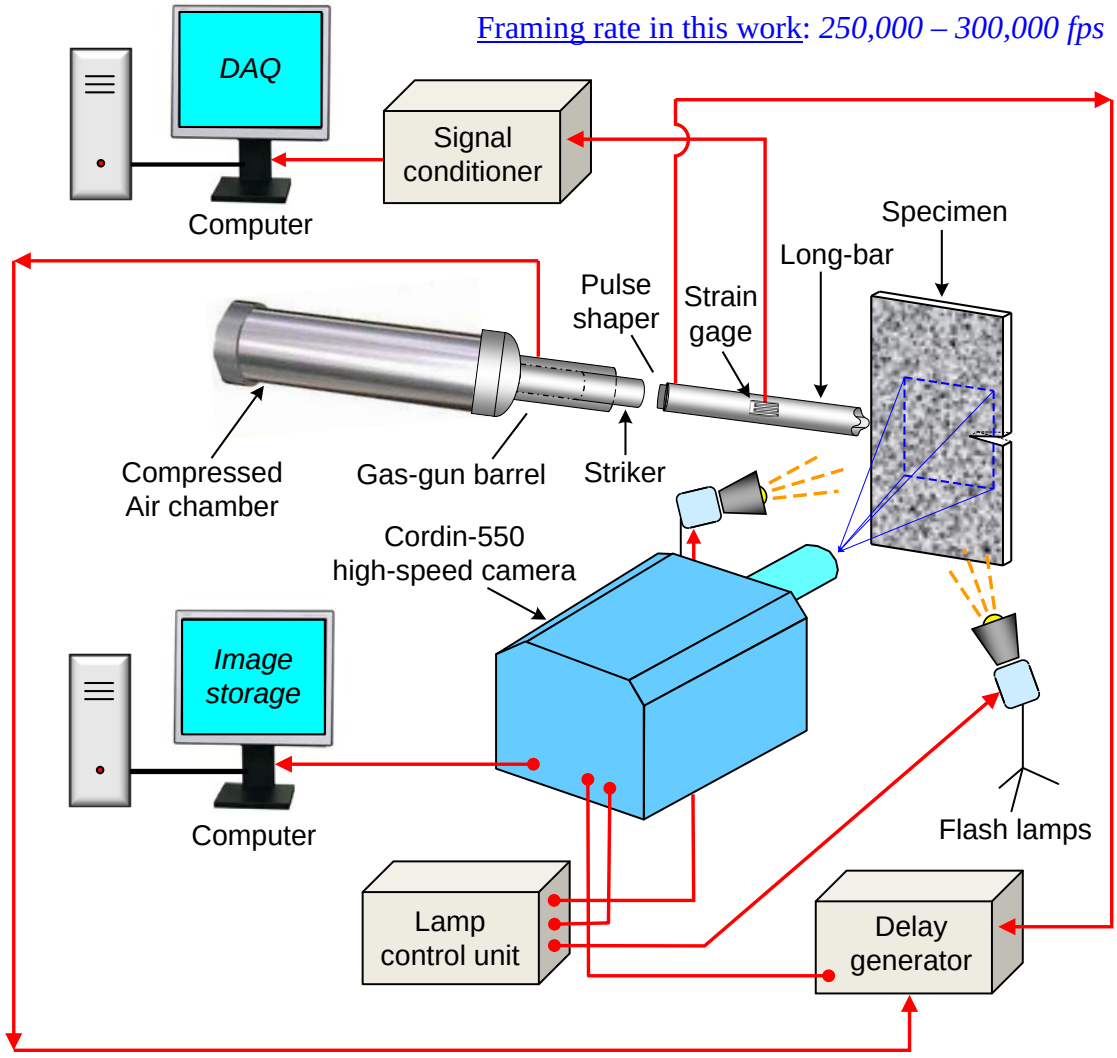

Figure 4 – Experimental set-up for testing high-strain mode-I fracture testing of *t*-IPNs. (in color)

A dynamic mode-I fracture set-up (Fig. 4) was developed to test high-strain rate fracture response of *t*-IPN materials. The set-up consists of a cylindrical striker (1" diameter and 12" long aluminum bar) propelled by a gas gun (impact velocity ~15-20 m/sec) to impact a long bar (8 feet long) to generate a stress pulse for a duration ~200 μsec. The other end of the long bar is shaped to produce a line contact with the specimen and is registered against the edge of an IPN sample (see close-up image in Fig. 5). The

surface texture (created in this case by spraying the IPN surface with mists of black and white paint) near the crack tip is photographed using an ultra-high-speed camera (UHS) at recording rates of ~300,000 frames per second. A few representative speckle images at various stages of fracture, before and after crack initiation, are shown in Fig. 6. The in-plane deformation histories are quantified from these images using 2D digital image correlation method by correlating deformed and undeformed speckle images.

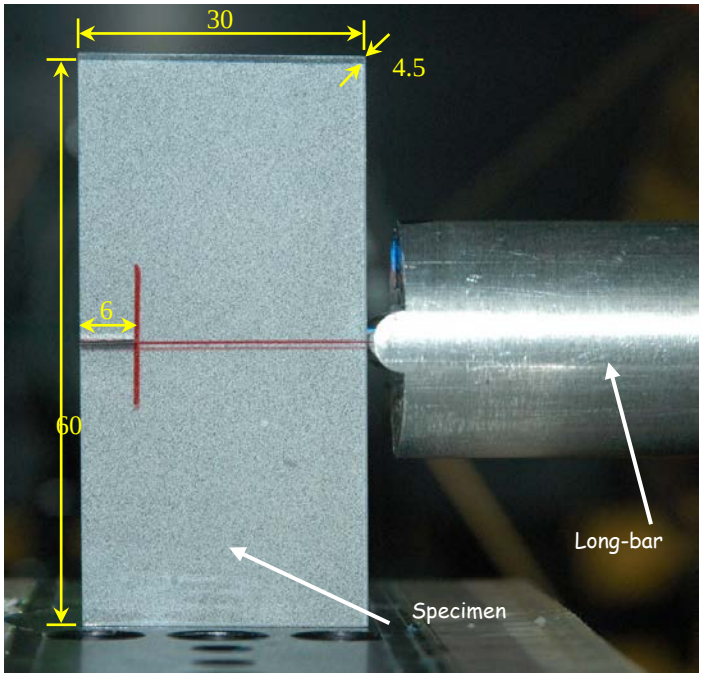

Figure 5 – Close-up view of mode-I specimen geometry used for fracture testing of *t*-IPNs. Dimensions in mm. (color photo)

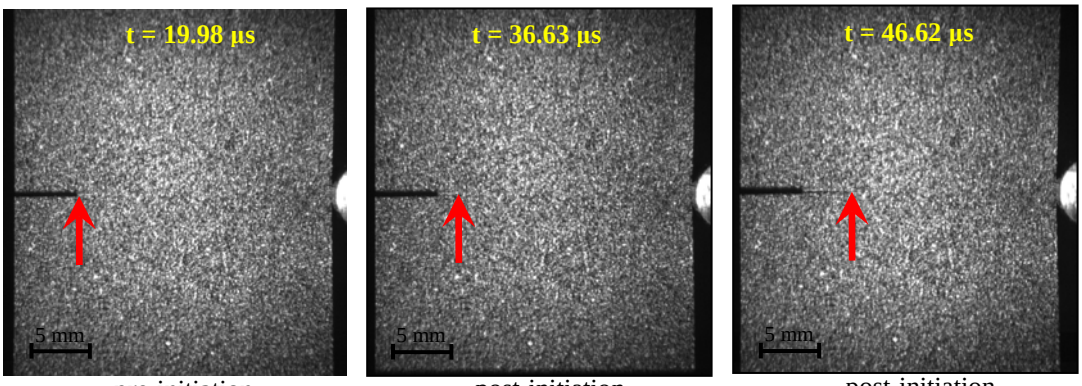

pre-initiation post-initiation post-initiation

Figure 6 – Speckle images (at a few select times after impact) in the crack tip vicinity of a PMMA sheet subjected to impact loading. The crack tip is located by the tip of the arrow in pre- and post-initiation regimes.

A few representative contours of constant crack opening displacements (displacements perpendicular to the crack) are shown in Fig. 7. Contours for three different IPNs, 90:10, 85:15

and 80:20, are shown with a contour interval of 7 μm between contours at different times after the start of the impact loading on the edge opposite to the crack. These displacement fields are analyzed in conjunction with mode-I crack tip equations under the assumption of small scale yielding to extract dynamic stress intensity factor (K_I) histories. The K_I histories are used to compare crack initiation toughness and crack growth performance of IPNs against commercial PMMA.

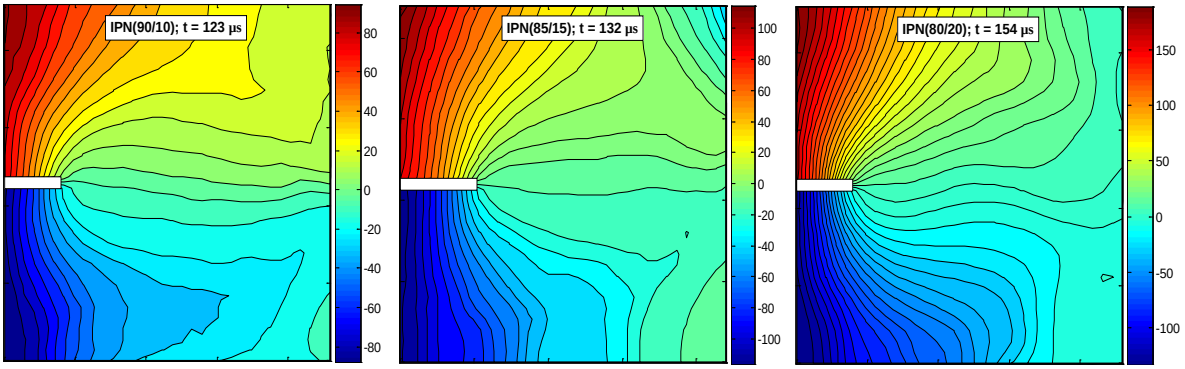

Figure 7 – Crack-opening (v-field) displacement contours for different IPNs. (Contour interval: 7 μm.) Color-bars indicate displacements in μm.

The crack velocity and stress intensity factor (K_I) histories for three IPNs are plotted in Figs. 8 and 9 along with the ones for commercial PMMA. *These results are for a new batch of IPN sheets cast in the past year. It is worth noting that sample preparation methodology has been*

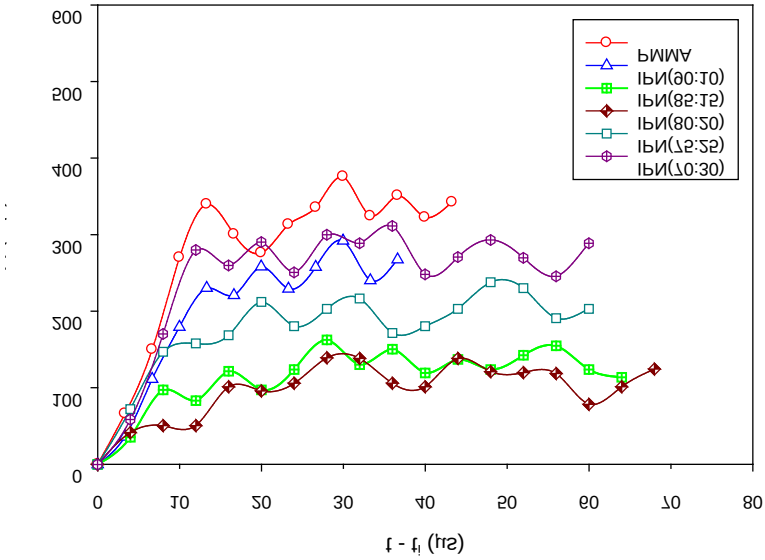

Figure 8 – Measured crack velocity histories for different IPNs. Crack initiation corresponds to (t-t_i) = 0 μs. (color plot)

improved in the past year to prevent vaporization of PMMA during IPN preparation, thereby the PMMA:PU ratio in the sample is close to the values at the start of the material preparation.

The steady state crack velocities (in the time window beyond rapid acceleration) for PMMA are the highest (300-350 m/sec) among all the specimens tested. On the contrary, IPN samples with PMMA:PU ratio of 85:15 and 80:20 show the least crack speeds (~100 m/sec). Further, for other compositions, the crack speed drops with increasing content of PU up to the composition ratio of 80:20 but begins to rise beyond this ratio. That is, 75:25 and 70:30 ratios show higher crack speeds when compared to 80:20 and 85:15 IPNs suggesting a change in the microstructure and hence the fracture mechanism.

The crack initiation toughness (corresponding to $t - t_i = 0$) initially increases with the PU content in the IPN. That is relative to PMMA, 90:10 and 85:15 show ~40% improvement (from ~1.6 MPa(m)$^{1/2}$ to ~2.25 MPa(m)$^{1/2}$) in K_I^d at crack initiation. However, as the PU content increased further, there is a precipitous drop in the crack initiation values in 80:20, 75:25, and 70:30 compositions. Furthermore, these trends continue into the post-initiation regime ($t - t_i > 0$). Based on these and the previously discussed velocity histories, an optimum IPN composition appears to be in the neighborhood of 85:15.

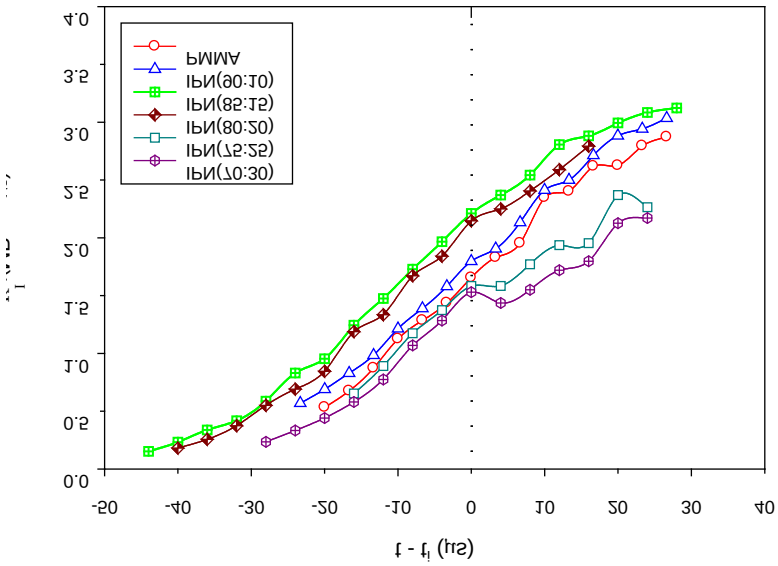

Figure 9 – Measured dynamic Stress intensity factor histories for different IPNs. Crack initiation toughness corresponds to K_I values at $(t\text{-}t_i) = 0$ μs. (color plot)

The fracture surface morphology from the dynamic fracture experiments were examined using SEM and a select few are shown in Fig. 10. PMMA fracture surface is nearly featureless a few conic (hyperbolic) markings, typical of neat brittle polymer fracture signifying low dissipation of fracture energy. On the contrary, IPN samples with *high* macroscale (apparent) dynamic crack initiation toughness show a noticeably textured/rugged surface with high roughness. The creation of these surface features involving fracture of PU and PMMA phases explains the high dynamic crack initiation toughness values seen in these IPNs. However, with increasing PU content, a fracture surface that resembles the one corresponding to low energy dissipation returns. These transitions in microscopic features are consistent with the drop in crack initiation toughness measured earlier. The basic mechanisms associated with this change in fracture

surface features are very likely due to phase inversion. That is, at low or high PU content, the fracture of IPNs is associated with either the PU phase acting as compliant inclusions in a brittle PMMA matrix or the brittle PMMA fillers in a compliant PU matrix. However, at optimum ratios of the two materials (such as 85/15, 80/20 at the chosen molecular weights), the two phases work synergistically resulting in deformation/ fracture/tearing of both the phases leading to maximum dissipation of energy.

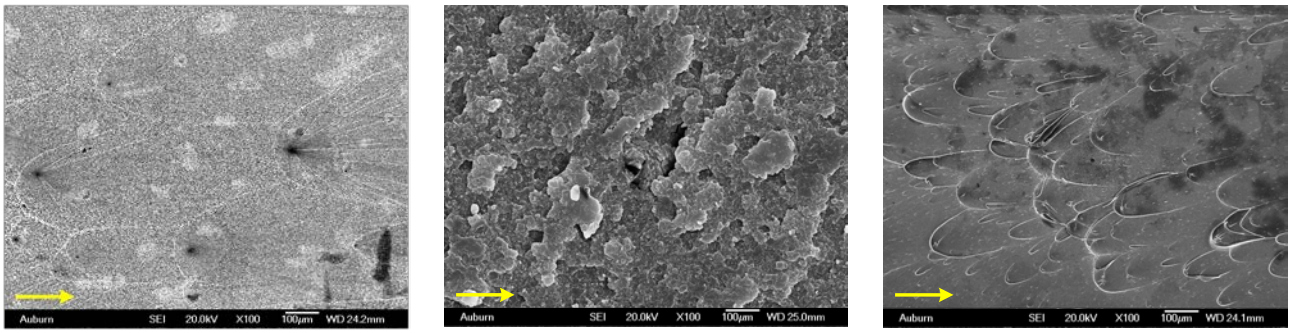

Figure 10 – SEM images of surface features of dynamically fractured specimens

Impact Energy Absorption:

To quantify the impact energy absorbed by IPNs of different composition in structural configurations, drop-tower tests are being carried out. A fixture to undertake impact tests using ASTM D5628-96 protocol has been constructed (see Fig. 11). The devise consists of a clamped plate (~110 mm diameter and 8-9 mm thick) made of IPN subjected to impact loading using a falling weight with a 12.5 mm hemispherical dart attachment. The instrumented dart assembly and the velocity history of the falling weight are used to measure energy dissipation during the dynamic event. Preliminary experiments suggest that a 4.5 m/sec impact velocity and 60 J of energy would be sufficient to fail both IPN and PMMA samples. The outcome these tests will be reported in the coming months.

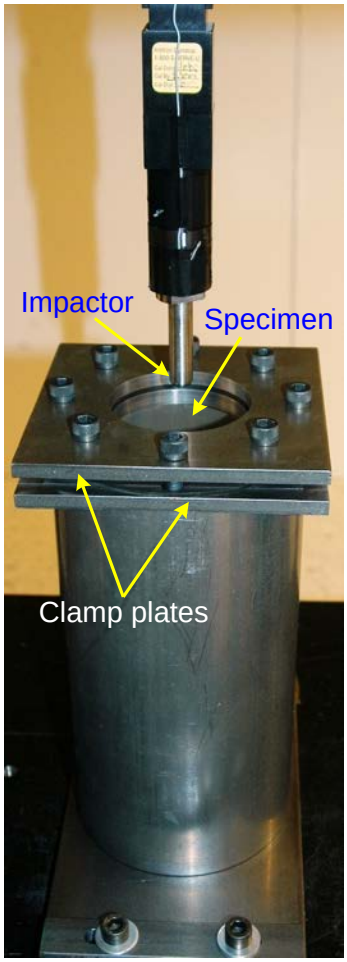

Figure 11 – Test fixture for IPN impact energy absorption studies.

IPNs Consisting of PMMA:PU with Various Molecular Weight Diols in the PU Phase

In order to enhance the material properties of the IPNs, the changes in the PU phase's network morphology and its subsequent effects were studied. For this section, the PU phase was altered by including diols of different molecular weight. The reactant used in the previous section for creating IPNs involved a 650g/mol diol. For this research, other molecular weights were explored: 1400g/mol, 2000g/mol, and 2900g/mol.

The procedure for synthesizing these IPNs was similar to the previous study, except PTMG/TRIOL mixtures varied, depending on which molecular weight diol was being utilized. All PU systems prepared were of the following equivalents: 0.19eq TRIOL: 0.12eq PTMG: 0.31eq DCH. These values were also used in the previous study. Both pure, cross-linked PU and IPNs with PMMA:PU ratios of 80:20 and 70:30 were synthesized.

Figure 12 shows the UV-vis results for IPNs consisting of 80:20 (PMMA:PU), shown in Figure 12a, as well as IPNs consisting of 70:30 (PMMA:PU), shown in Figure 12b, with diols of various molecular weight.

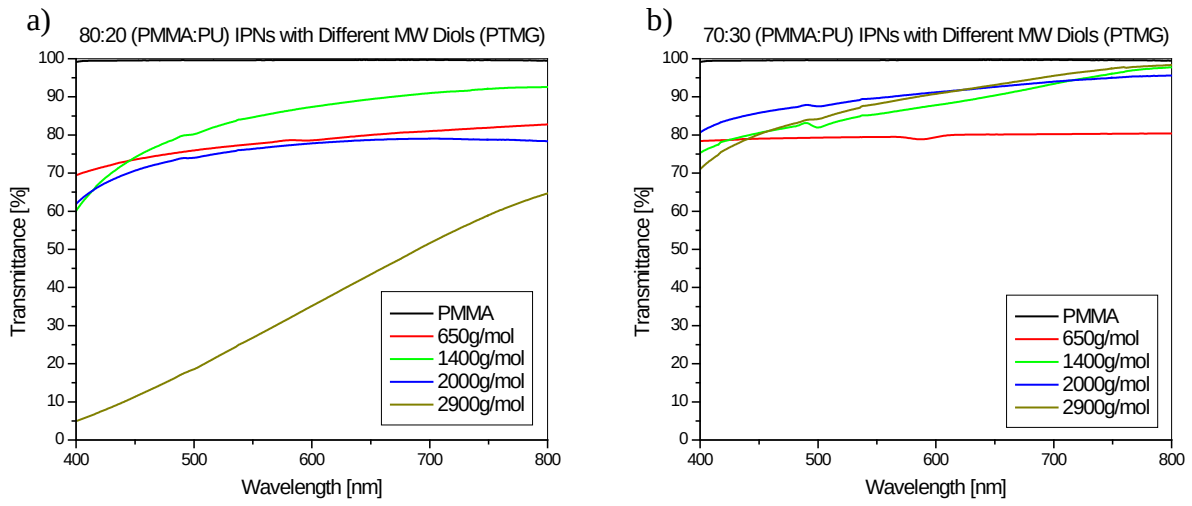

Figure 12. Transparency results from UV-vis analysis for IPNs with different diols in the PU phase with ratios of a) 80:20 (PMMA:PU) and b) 70:30 (PMMA:PU)

For the graphs, commercial PMMA was also included as a reference. As can be seen from looking at the graphs, the IPNs did not quite have the transparency values as high as commercial PMMA; however, the transparency was still relatively high, especially for materials with 1400g/mol. IPNs with 2900g/mol PTMG, on the other hand, showed poor values of transparency.

It was also interesting to note that samples with 70:30 (PMMA:PU) had better values of transparency than IPNs consisting of 80:20 (PMMA:PU). This was indicative that phase separation may have been present more in IPNs with this particular weight ratio.

The morphologies of the IPNs were further investigated by studying their domains with the TEM. Similar to the previous study, the IPNs were stained with osmium tetroxide, and the PMMA phase remained unstained while the PU phase absorbed the dye. Thus, distinguishing between the two phases under the microscope was possible. TEM photos of IPNs with various diols in the PU phase can be seen in Figure 13.

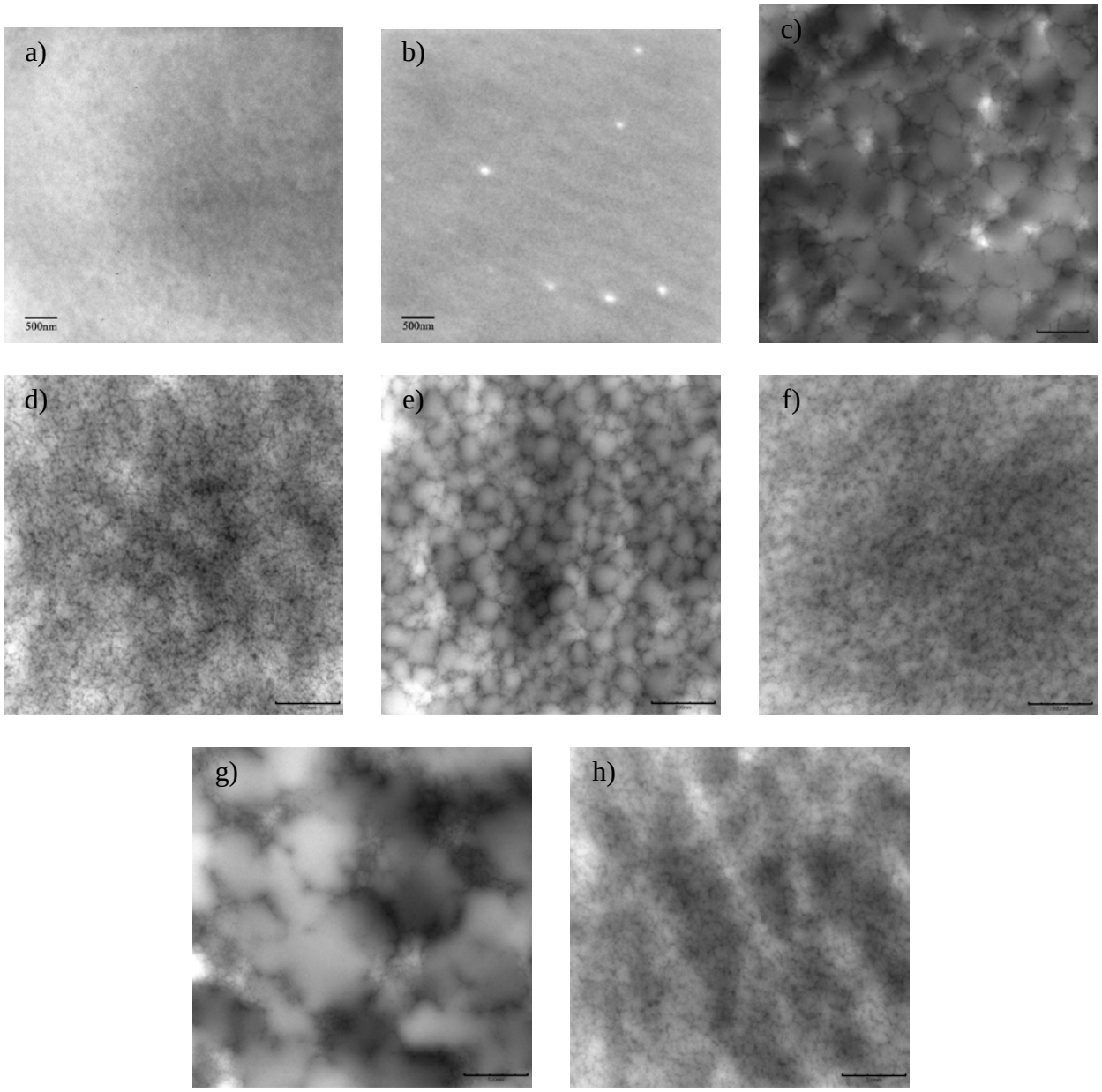

Figure 13. TEM photos of IPNs (PMMA:PU) with diols of molecular weights a) 650g/mol (80:20), b) 650g/mol (70:30), c) 1400g/mol (80:20), d) 1400g/mol (70:30), e) 2000g/mol (80:20), f) 2000g/mol (70:30), g) 2900g/mol (80:20), and h) 2900g/mol (70:30)

The larger domains evidenced in the TEM photos for IPNs with the PMMA:PU ratio of 80:20 confirm slight phase separation did take place, which ultimately decreased the transparency.

Another aspect to note is the increase in the domain sizes as the molecular weight of the diol used in the PU phase increased. A higher molecular weight diol correlates to a longer chain length, and this created PU networks with increased areas within the domains. This also translates into more PMMA being able to swell in between the PU network. The corresponding molecular weight between cross-links and cross-link density of the IPNs, determined by pycnometer and swelling experiments, can be seen in Table 1.

Table 1. Molecular weights between cross-links and cross-link densities for pure, cross-linked PU samples and IPNs consisting of diols of various molecular weights

(PMMA:PU)	**Molecular Weight between Cross-links (g/mol)**	**Cross-link Density (mol/mL)**
650g/mol Pure PU (0:100)	129.77	4.84×10^{21}
650g/mol 70:30	258.84	2.54×10^{21}
650g/mol 80:20	258.10	2.37×10^{21}
1400g/mol Pure PU (0:100)	231.33	2.70×10^{21}
1400g/mol 70:30	971.79	6.99×10^{20}
1400g/mol 80:20	347.27	2.00×10^{21}
2000g/mol Pure PU (0:100)	270.33	2.35×10^{21}
2000g/mol 70:30	488.07	1.41×10^{21}
2000g/mol 80:20	246.25	2.66×10^{21}
2900g/mol Pure PU (0:100)	861.32	7.00×10^{20}
2900g/mol 70:30	1118.11666	5.96×10^{20}
2900g/mol 80:20	310.49212	2.278×10^{21}

As can be seen from the table, the molecular weight between cross-links increased and the cross-link density decreased for samples with a high molecular weight. This was expected since including a longer chain diol in the PU phase should increase the chain length and the molecular weight between cross-links. Concurrently, the number of cross-links in a given area, or the cross-link density, would be lower than other samples. Additionally, IPNs with the PMMA:PU ratio of 70:30 were able to swell more than their 80:20 or pure, cross-linked PU counterparts. This may be due to the pure PU being able to cross-link freely with no restrictions, whereas PU paired with PMMA in an IPN would restrict the number of cross-links that could form.

Finally, the thermo-mechanical and fracture properties from using different molecular weight diols were investigated. E' and T_g values obtained from DMA tests can be seen in Table 2.

Table 2. E' and T_g values for IPNs with different molecular weight diols

Molecular Weight	**PMMA:PU**	**E' [GPa] (30°C)**	**T_g [°C]**
650g/mol	80:20	1.02 ± 1.3	119.98 ± 19.77
	70:30	0.75 ± 0.68	102.62 ± 15.45
1400g/mol	80:20	0.73 ± 0.11	129.67 ± 3.15
	70:30	0.37 ± 0.14	110.05 ± 0.98
2000g/mol	80:20	0.85 ± 0.31	133.20 ± 2.88
	70:30	0.36 ± 0.17	120.98 ± 9.25

2900g/mol	80:20	0.82 ± 0.23	143.78 ± 1.48
	70:30	0.44 ± 0.01	124.14 ± 3.16

It was initially expected that E' would decrease when diols of higher molecular weights were incorporated into the PU phase and the IPN. However, the E' generally remained constant. Further analysis with differential scanning calorimetry (DSC) revealed that IPNs with a diol of 2000g/mol or higher exhibited crystallinity within its structure. The crystalline regions therefore acted as reinforcement and increased the stiffness of the materials.

The T_g of the IPNs also increased with higher molecular weight diols. This may be due to the phase separation seen earlier in the TEM photos. These higher values of T_g may actually correspond to the PMMA phase present in the IPN. With good miscibility between the two phases, the T_g would have shifted more to lower temperatures, closer to that of PU's T_g. However, since phase separation took place, the T_g of the samples increased.

IPNs Consisting of PMMA:PU with Various Chain Flexibilities in the PU Phase

For the next part of this project, the PU phase was altered in a different way with the purpose of, again, enhancing the material properties of the IPN. The PU network was modified by changing the ratio of PTMG to TRIOL while still using the 650g/mol PTMG, similar to the first section in this research. Table 3 shows the equivalent values used and the corresponding chain flexibilities of the PTMG/TRIOL mixtures, which are basically the ratios of the amount of diol to triol. In other words, a higher percent chain flexibility meant more diol was present.

Table 3. Equivalent values and corresponding chain flexibilities used for this study

TRIOL	**PTMG**	**DCH**	**Chain Flexibility**
0.19eq	0.12eq	0.31eq	19.35%
0.12eq	0.19eq	0.31eq	30.65%
0.06eq	0.25eq	0.31eq	40.32%
0.00eq	0.31eq	0.31eq	100% (linear)

As in the previous studies, synthesis of the IPNs was the same, except for which PTMG/TRIOL mixture was used. IPN samples synthesized included these chain flexibilities and PMMA:PU ratios of 80:20 and 70:30. TEM photos of various IPNs can be seen in Figure 14.

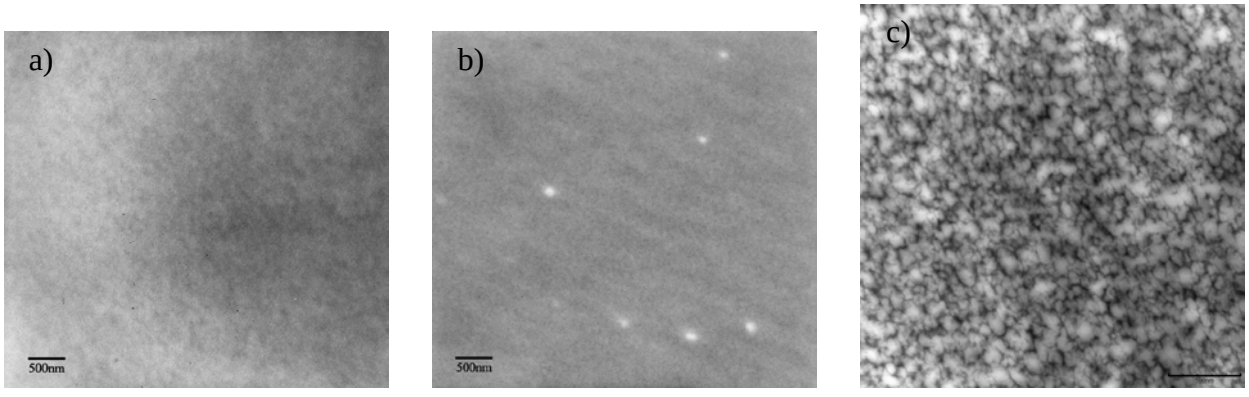

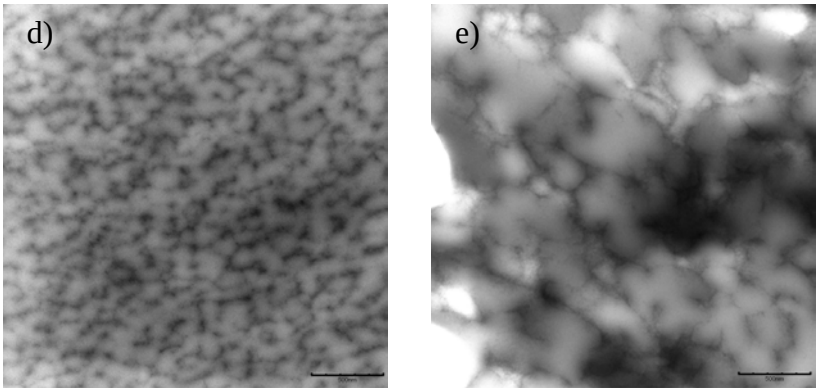

Figure 14. TEM photos of IPNs (PMMA:PU) with flexibilities of a) 19.35% (80:20), b) 19.35% (70:30), c) 30.65% (80:20), d) 40.32% (80:20), and e) 40.32% (70:30)

From the TEM, it seemed that IPNs with a higher percent chain flexibility displayed increasingly more distinct domains. In other words, phase separation became more imminent because if the samples showed better compatibility between the phases, then the TEM would show a more homogeneous structure.

In order to get a better understanding of the morphology of the samples the molecular weight between cross-links and the cross-link densities were also calculated for pure, cross-linked PU and IPN samples with different chain flexibilities. The results after calculations from pycnometer and swelling experiments can be seen in Table 4.

Table 4. Molecular weights between cross-links and cross-link densities for pure, cross-linked PU samples and IPNs consisting of diols of various chain flexibilities

Sample (PMMA:PU)	**Molecular Weight between Cross-links [g/mol]**	**Cross-link Density [g/mol]**
19.35% (0:100) – Pure PU	129.77	4.84×10^{21}
19.35% (70:30)	258.84	2.54×10^{21}
19.35% (80:20)	258.10	2.37×10^{21}
30.65% (0:100) – Pure PU	163.27	3.78×10^{21}
30.65% (70:30)	473.80	1.51×10^{21}
30.65% (80:20)	371.11	1.83×10^{21}
40.32% (0:100) – Pure PU	443.16	1.34×10^{21}
40.32% (70:30)	514.70	1.33×10^{21}
40.32% (80:20)	15.33	4.15×10^{22}

The same phenomenon that was observed in the previous study with the different molecular weight diols in the PU phase was also observed for the pure, cross-linked PUs and the IPNs with different chain flexibilities. The molecular weight between cross-links was highest and the cross-link density was lowest for samples with 30 wt% PU. It is possible that in this case, the pure, cross-linked PU was cross-linked more than the than the IPNs, which restricted how much

it could swell. However, with the presence of PMMA in the IPN, the cross-linking abilities of PU were disrupted by PMMA chains, thus allowing the IPNs to swell more. Furthermore, having 30 wt% versus 20 wt% of the flexible phase, the IPNs were capable of swelling even more. This may correspond to having more of the flexible phase in an IPN would allowe the IPN to swell even more.

One aspect that should be noted is the relatively higher values of molecular weight between cross-links and the much lower cross-link densities for samples with 40.32% chain flexibility. Perhaps the high molecular weight between cross-links is the reason why some phase separation took place for these IPNs.

Other parameters investigated for these systems included the thermo-mechanical properties, such as E' and T_g. Figure 15 shows these values for IPNs with different chain flexibilities.

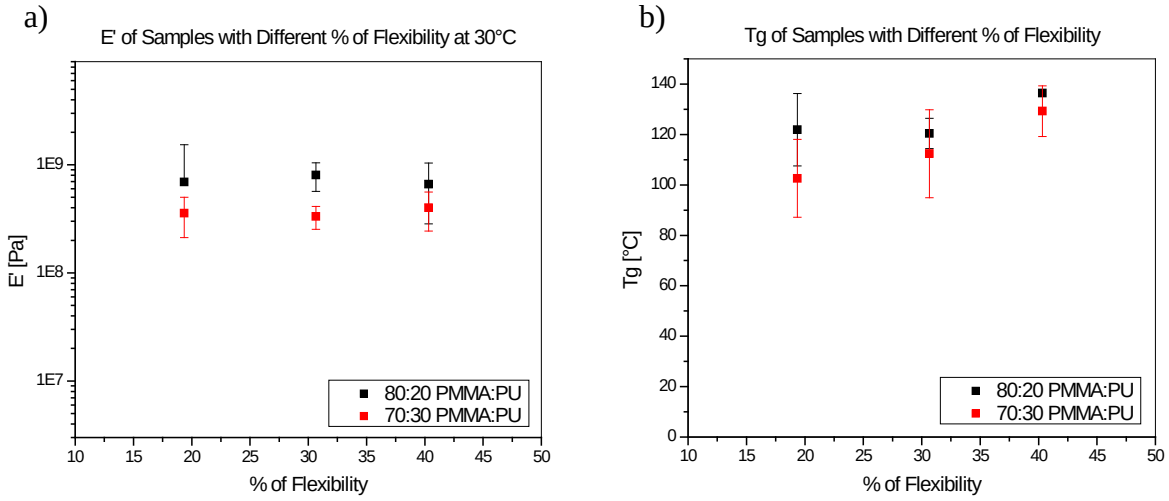

Figure 15. DMA results showing a) E' and b) T_g values of IPNs with different chain flexibilities

According to Figure 15b, the T_g of the IPNs increased when a higher chain flexibility in the PU phase was used. This was similar to the trend seen in the previous study with the different molecular weight diols. Since phase separation became more prominent with the higher chain flexibilities, this could mean that the T_g that was observed in the graph actually corresponds to the T_g of the PMMA phase.

Looking more at Figure 8, there appeared to be no significant change in the E' values. This was not initially expected since having a more flexible PU phase would have translated into having a more flexible IPN. Again, using DSC analysis similar to the last study, it was found that cold crystallization had taken place, which acted as reinforcement for the IPNs. Therefore, as the flexibility increased, more crystallization took place, which is why the E' values did not significantly change. The DSC results of the IPNs showing the cold crystallization temperatures (Tcc) and corresponding enthalpies can be seen in Table 5.

Table 5. Cold crystallization temperatures and correlating enthalpies for pure, cross-linked PU and IPNs with different chain flexibilities

Sample	Chain Flexibility	Ratio	T_{cc} [°C]	ΔH [J/g]
Pure cross-linked PU	19.35%	0:100	-	-
	30.65%	0:100	-	-
	40.32%	0:100	-3.93	8.75
IPN	19.35%	70:30	-	-
		80:20	-	-
	30.65%	70:30	Not tested	Not tested
		80:20	26.94	4.706
	40.32%	70:30	22.02	42.26
		80:20	24.12	32.59

Fracture tests are currently being performed to determine the fracture toughness of these IPNs.

IPNs Consisting of PMMA:PU with Silica Nanoparticle Reinforcement

Another objective of this research was the inclusion of organic silanes, eventually silica particles, in the *t*-IPNs. Different approaches have been taken for incorporating these fillers, in order to achieve added reinforcement. The first technique involved synthesizing silica particles outside of the IPN, and then later introducing the particles into the IPNs through physical mixing. For this technique, the following chemicals were used: ammonium hydroxide, ethanol, deionized water, and tetraethyl orthosilicate (TEOS). In order to create these materials, the same procedures for synthesizing and curing the IPNs were followed from before, but just before curing, the silica particles were added, sonicated, and mixed until a homogenous solution was achieved.

Figure 16 shows results of light scattering analysis for determining the diameters of the silica particles that were formed. Clearly, the ratio of ammonium hydroxide to water plays a crucial role in the size of the particles. When the silica precursor consisted of 10mL of ammonium hydroxide, particles over 800nm in diameter were produced, which is no longer considered in the nanoscale range. However, when a lesser amount of ammonium hydroxide was included, such as 1mL, the diameter drastically decreased to around 200nm.

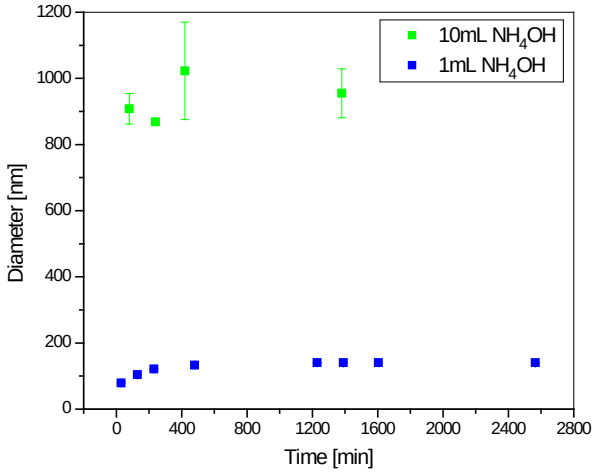

Figure 16. Light scattering results showing different diameters created by varying the ratio of ammonium hydroxide to water.

When using a lesser amount of ammonium hydroxide the uniformity of the particles also greatly improved. The picture in Figure 17 shows a photo using a transmission electron microscope (TEM) of actual particles that were synthesized and added to the IPN systems. As can be seen, the particles, while not exactly uniform in shape, appear to be spherical. Creating smaller particles more uniform in shape and size is still being investigated.

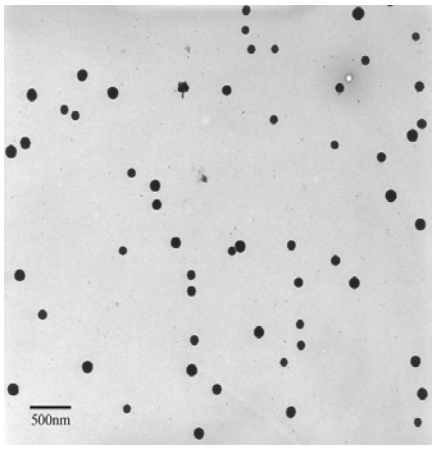

Figure 17. TEM picture of silica particles developed using ammonium hydroxide, ethanol, deionized water, and tetraethyl orthosilicate. These particles were placed directly into the IPN before curing.

Figure 18 shows some dynamic mechanical analysis (DMA) results for a 90:10 (PMMA:PU) IPN sample that was synthesized with particles from the 1mL ammonium hydroxide solution. The IPN consisted of an inhibitor in the PMMA phase and DCH in the PU phase.

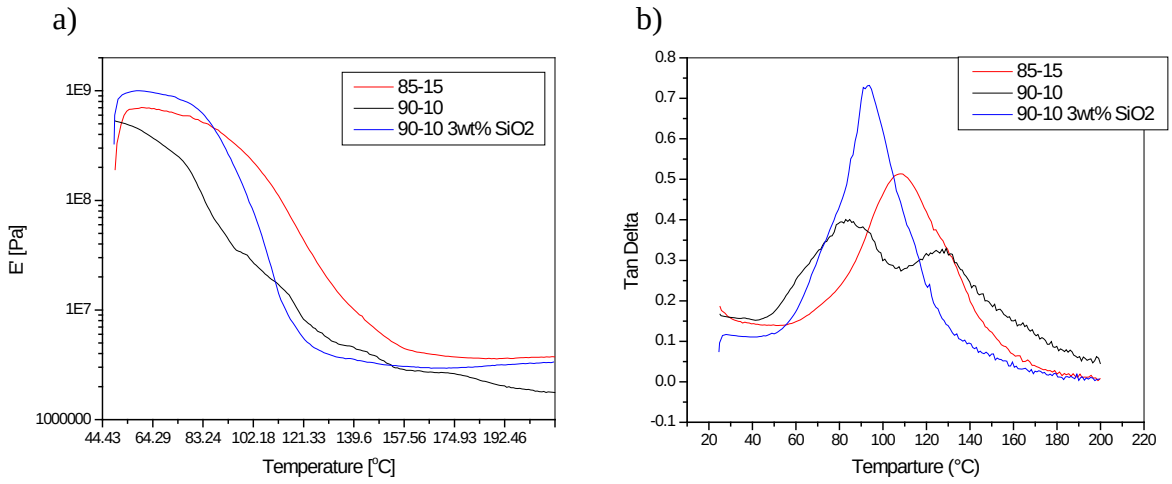

Figure 18. DMA results showing the Young's modulus (a) and T_g (b) of the IPN systems with the silica particles included.

Although the Young's modulus (stiffness) of the materials is still in the GPa range and the glass transition temperature (T_g) is also relatively high, the sample displayed similar mechanical properties as samples without silica reinforcement. This similarity could result from a poor dispersion of the silica particles; thus, studies in understanding how to achieve a better dispersion are in progress.

Another approach in the reinforcement of the IPNs was the in situ development of silica particles. For this, the following chemicals were used: 3-(Trimethoxysilyl)propyl methacrylate)

(TMSPM), (3-Isocyanatopropyl)triethoxysilane (IPTES), distilled water, and hydrochloric acid. Creating these systems involved mixing the PMMA and PU precursors together, without the DD. Next, the TMSPM and IPTES, either together or separately in different samples, were added drop wise. The DD was then added, and the solution was mixed. Afterwards, the hydrochloric acid and distilled water were added, the solution was mixed again, and then the samples were placed into the oven for the same curing treatment as before.

The scanning electron microscope (SEM) photo in Figure 19 shows a typical sample with TMSPM and IPTES in an IPN. This photograph was taken after the sample was broken at liquid nitrogen temperatures, or during brittle failure. From this picture, it is possible to see the different domains within the sample.

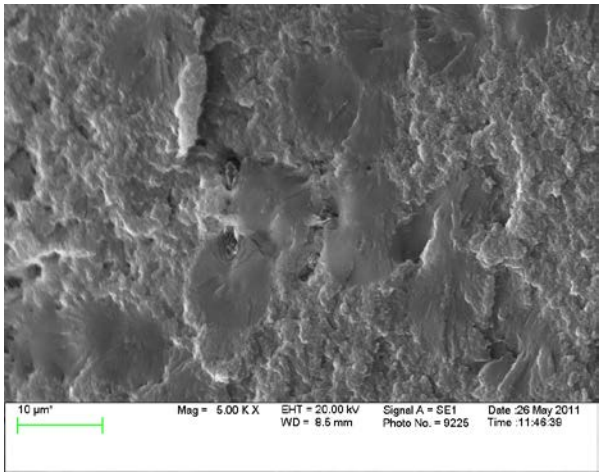

Figure 19. SEM photo of surface morphology of a sample with IPTES and TMSPM after brittle failure.

Personnel Supported:

List professional personnel (Faculty, Post-Docs, Graduate Students, etc.) supported by and/or associated with the research effort.

Dr. Hareesh V. Tippur
Professor of Mechanical Engineering, Auburn University

Dr. Maria L. Auad
Professor of Polymer and Fiber Engineering Department, Auburn University

Students:
Dan Clary (May 15, 2009 - August 15, 2009)
Samantha Bird (August 15, 2009 – July 31, 2013)
Kailash Jajam (July 15, 2009 - July 31, 2013)

Undergraduate Student
Andrea Alexander (August 2010 - March 31, 2013)

Publications:

List peer-reviewed publications and theses submitted and/or accepted during the project period:

- 'Interpenetrating Polymer Networks with Polyurethane and Methacrylate-based Polymers,' S. A. Bird, PhD Dissertation, Department of Polymer and Fiber Engineering, Auburn University, Summer 2013.

- 'Fracture Behavior of Particulate Polymer Composites and Interpenetrating Polymer Networks,' K. C. Jajam, PhD Dissertation, Department of Mechanical Engineering, Auburn University, Summer 2013.

- 'Development and Characterization of a PU-PMMA Transparent Interpenetrating Polymer Networks (*t*-IPNs),' K. C. Jajam, H. V. Tippur, S. Bird and M. L. Auad, Proceedings of SEM Annual Conference, Uncasville, CT, June 2011. (paper #334) [Dynamic Behavior of Materials, Vol. 1, pp 117-121, 2011, Springer publications]

- "Synthesis and characterization of high performance, transparent interpenetrating polymer networks with polyurethane and poly(methyl and methacrylate)", Bird SA, Clary D, Jajam KC, Tippur HV, Auad ML., *Polymer Engineering and Science*, Vol. 53, No. 4, pp 716-723, 2013

- "Development of a Molecular Interpenetrating Polymer Composite using an Acrylate-based Copolymer and Polyurethane", Master's Graduate Project, Master Polymer and Fiber Eng., Samantha Bird. July 14, 2011

- 'Tensile, Fracture and Impact Behavior of Transparent Interpenetrating Polymer Networks with Polyurethane-poly(methyl methacrylate),' K. C. Jajam, S. A. Bird, M. L. Auad, and H. V. Tippur, *Polymer Testing*, Vol. 32, pp 889-900, 2013.

- 'Dynamic fracture and impact energy absorption characteristics of transparent interpenetrating PU-PMMA polymer networks,' K.C. Jajam, H.V. Tippur, S.A. Bird, M.L. Auad , paper # 208, 2013 SEM Annual Conference, June 2013, Lombard, IL.

- 'Fracture and Impact Energy Absorption Characteristics of PMMA-PU Transparent Interpenetrating Polymer Networks,' K. C. Jajam, H. V. Tippur, S. A. Bird, and M. L. Auad, Proceedings of the 50th SES Annual Technical Meeting and ASME-AMD Summer Meeting, Providence, RI, July 2013.

Interactions/Transitions:

a. Participation/presentations at meetings, conferences, seminars, etc.

- "Synthesis and Characterization of High Performance, Transparent Interpenetrating Polymer Networks with Poly(methyl methacrylate) and Polyurethane with Diols of Varying Molecular Weight." S. A. Bird, K. C. Jajam, A. C. Alexander, H. V. Tippur, M. L. Auad. Alabama Composites Conference, University of Alabama at Birmingham, AL, 19 June 2013. Poster Presentation.

- "Development of Transparent and High Performance Interpenetrating Polymer Networks." Graduate Scholars Forum, Auburn University, AL, 1 March 2011. Presentation.

- "Molecular Interpenetrating Polymer Composites using Acrylate-based Polymers and Polyurethane." S. A. Bird, K. C. Jajam, M. L. Auad. H. V. Tippur, Graduate Student Research Showcase, Auburn University, AL, 13 September 2012. Poster Presentation.

- "Synthesis and Characterization of High Performance, Transparent Interpenetrating Polymer Networks with Polyurethane and Poly(methyl methacrylate) with Different Polyurethane Network Morphologies." S. A. Bird, M. L. Auad. Graduate Scholars Forum, Auburn University, AL, 26 February 2013. Presentation.

- "Development of Transparent and High Performance Interpenetrating Polymer Networks with Polyurethane and Poly(methyl methacrylate)." Master's Presentation, Spring 2011.

- DTRA Basic Research Technical Review (BRTR) (Oct 2009, August 2010, July 2011), Arlington, VA.

- "Interpenetrating Polymer Networks", S.A. Bird, M. L. Auad, Society of Plastic Engineering (SPE-ANTEC), Orlando Florida, (April, 2012)

- Poster presentation during Graduate Scholars Forum, S. A. Bird, Auburn University, Alabama (September, 2012)

b. Consultative and advisory functions to other laboratories and agencies and other DoD laboratories. Provide factual information about the subject matter, institutions, locations, dates, and name(s) of principal individuals involved.

None

c. Transitions. Describe cases where knowledge resulting from your effort is used, or will be used, in a technology application. Transitions can be to entities in the DoD, other federal agencies, or industry. Briefly list the enabling research, the laboratory or company, and an individual in that organization who made use of your research.

None

New discoveries, inventions, or patent disclosures:

- U.S. Provisional Patent Application No. 61/506,824 entitled "Transparent Interpenetrating Polymer Network Based on Poly(Methyl Methacrylate) / Polyurethane Networks" Inventor(s): Maria L. Auad, Hareesh V. Tippur, Dan Clary, Samantha A. Bird, Kailash Jajam. Filing Date: 7/12/2011 (AU Invention No. 2010-081)

Honors/Awards:

List honors, degrees, and awards received during the grant/contract period. List lifetime achievement honors such as Nobel prize, honorary doctorates, and society fellowships prior to this effort.

- Samantha Bird - Master of Science (Non-Thesis), Summer 2011
- Kailash Jajam – Harry Merriwether Fellowship for Academic Excellence and Scholarly Achievement, Auburn University, Graduate School (2012)
- Kailash Jajam – Outstanding International Graduate Student Award in Mechanical Engineering, Auburn University (2012)
- Maria Auad – Tenured & Promoted as Associate Professor, Auburn University, AL, Fall 2011
- Hareesh Tippur – Fellow, Society for Experimental Mechanics (June 2011)
- Hareesh Tippur – W. F. Walker Teaching Award for Excellence, College of Engineering, Auburn University, 2012.
- Kailash Jajam and Hareesh Tippur – Best Paper Award, 2012 SEM XII International Congress on Experimental and Applied Mechanics, Costa Mesa, CA.

DEPARTMENT OF DEFENSE

DEFENSE THREAT REDUCTION AGENCY
8725 JOHN J. KINGMAN ROAD
STOP 6201
FORT BELVOIR ,VA 22060
ATTN: C. SHIPBAUGH

DEFENSE THREAT REDUCTION AGENCY
8725 JOHN J. KINGMAN ROAD
STOP 6201
FORT BELVOIR ,VA 22060
ATTN: M. ROBINSON

DEFENSE TECHNICAL INFORMATION CENTER
8725 JOHN J. KINGMAN ROAD,
SUITE 0944
FT. BELVOIR, VA 22060-6201
ATTN: DTIC/OCA

DEPARTMENT OF THE ARMY

ARMY RESEARCH LABORATORY
2800 POWDER MILL ROAD
ADELPHI , MD 20783
ATTN: DR. J.M. SANDS

ARMY RESEARCH LABORATORY
2800 POWDER MILL ROAD
ADELPHI , MD 20783
ATTN: DR. A. HSIEH

ARMY RESEARCH LABORATORY
2800 POWDER MILL ROAD
ADELPHI , MD 20783
ATTN: P. DEHMER

DEPARTMENT OF DEFENSE CONTRACTORS

EXELIS, INC.
1680 TEXAS STREET, SE
KIRTLAND AFB, NM 87117-5669
ATTN: DTRIAC

AUBURN UNIVERSITY
DEPARTMENT OF MECHANICAL ENGINEERING
AUBURN, AL 36849
ATTN: DR. H.V. TIPPUR

AUBURN UNIVERSITY
DEPARTMENT OF POLYMER AND FIBER ENGINEERING
AUBURN, AL 36849
ATTN: DR. M.L. AUAD